Electronic Supplementary Information

A dendrite-suppressed Li composite anode decorated by lithiophilic Li-Pb alloys for stable Li metal batteries

Jing Bai,[‡a] Ziwei Zhu, [‡a] Xue Liu,[a] and Sheng Liu*[a]

Institute of New Energy Material Chemistry, School of Materials Science and Engineering, Nankai University, Tianjin 300350, China. E-mail: shengliu@nankai.edu.cn.

1. Experimental Section

Fabrication of the Li-Pb alloy electrodes: The composite electrodes were fabricated by using a mechanical rolling method. Specifically, after polishing with a soft brush, Li foils and Pb foils in the atomic ratio of 88:5 were stacked in the sequence of Li-Pb-Li, followed by folding and roller pressing under a pressure of 4 tons in an Ar-filled glovebox. This process was repeated 20 times for full compounding between Li and Pb. Finally, the obtained composite sheet with a thickness of 500 μm was punched into round electrode plates with a diameter of 14 mm.

Preparation of the $Li_4Ti_5O_{12}$ electrodes: To assemble the full cells, $Li_4Ti_5O_{12}$ (LTO) electrodes were fabricated. The LTO electrode slurry was prepared by mixing $Li_4Ti_5O_{12}$ (Shenzhen Kejing Star Co.), conductive carbon (Super P) and polycinylidene fluoride (PVdF) (8:1:1 by weight ratio) in N-methylpyrrolidone (NMP). After stirring for 5 hours, the slurry was coated with a thickness of 75 μm on a clean copper foil, followed by drying at 100 ℃ for 12 h and punching into round electrode plates with a diameter of 10 mm.

Materials characterizations: X-ray diffractometer (XRD, Rigaku mini Flex II) was employed to test the phase composition of the samples with Cu Kα1 radiation (λ = 0.15405 nm), and the scanning

range (2θ) of patterns was 5-85° with a controlled scanning speed (4° min^{-1}). The morphologies of Li metals and Li-Pb alloy electrodes as well as the element distribution of Li-Pb alloy electrodes were characterized by using a scanning electron microscope (SEM, Supra 55VP, Zeiss) equipped with the energy dispersive spectrometry (EDS) system. The distribution of Li and Pb in the Li-Pb composite electrodes was analyzed by laser-induced breakdown spectroscopy (LIBS, ASI J200) within an area of 4.5 mm × 4.5 mm. Lithium dendrite growth on Li and Li-Pb composite electrodes was monitored in a transparent optical cell using optical microscopy (Nikon SMZ800N). The X-ray photoelectron spectra (XPS, Thermo Scientific ESCALAB 250Xi) were carried out to analyze the chemical composition of SEI.

Electrochemical tests: Coin-type cells (2032) were assembled in glovebox filled with argon atmosphere ($O_2 \leq 0.1$ ppm, $H_2O \leq 0.1$ ppm) to evaluate the electrochemical performance. The symmetric cells and full cells were assembled with Clegard 2300 as the separator and 40 μL electrolyte for each cell. The electrolyte consists of 1 M lithium bis (trifluoromethanesulfonyl) imide (LiTFSI) and 0.2 M $LiNO_3$ as additive in 1,2-dimethoxyethane (DME) and 1,3-dioxolane (DOL) (1:1 by volume). Electrochemical impedance spectra (EIS) were performed on a Zahner IM6ex electrochemical workstation with a frequency range of 10 mHz to 100 kHz and an amplitude of 5 mV. The symmetric cells of Li/Li and Li-Pb/Li-Pb were assembled to explore the stripping/plating behavior of lithium and monitor the changes in voltage polarization during long-term galvanostatic cycles with a capacity of 1 mAh cm^{-2} under various current densities (0.2, 0.5 and 5 mA cm^{-2}). The long-term cycling stability of the different electrodes in symmetrical cells was evaluated with a higher capacity of 5 mAh cm^{-2} at 5 mA cm^{-2}. The full cells of Li/LTO and Li-Pb/LTO were assembled and cycled at 1 C rate to obtain the charge-discharge curves and cycling performance of

different anodes. The cutoff potentials for discharge and charge were 1.0 and 2.2 V, respectively. All discharge/charge tests were carried out with LAND-CT2001A instruments (Wuhan Jinnuo, China).

2. Supporting figures

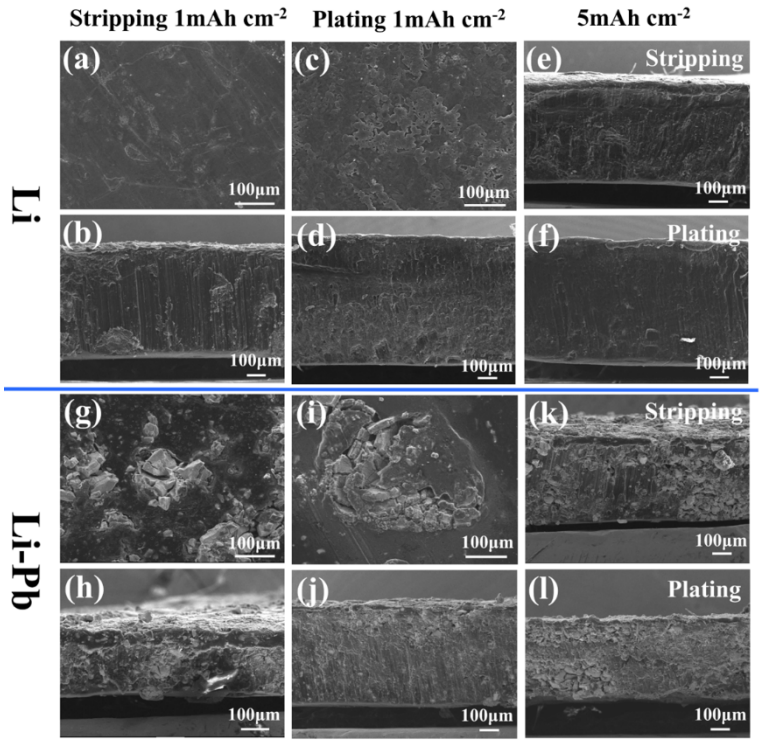

Fig. S 1 Top view SEM images of Li and Li-Pb alloy electrodes after stripping lithium for 1 mAh cm^{-2} (a, g); Cross-sectional SEM images of Li and Li-Pb alloy electrodes after stripping lithium for 1 mAh cm^{-2} (b, h), 5 mAh cm^{-2} (e, f); Top view SEM images of Li and Li-Pb alloy electrodes after plating lithium for 1 mAh cm^{-2} (c, i); and Cross-sectional SEM images of Li and Li-Pb alloy electrodes after plating lithium for 1 mAh cm^{-2} (d, j), 5 mAh cm^{-2} (f, l). The current density is fixed at 0.5 mA cm^{-2}.

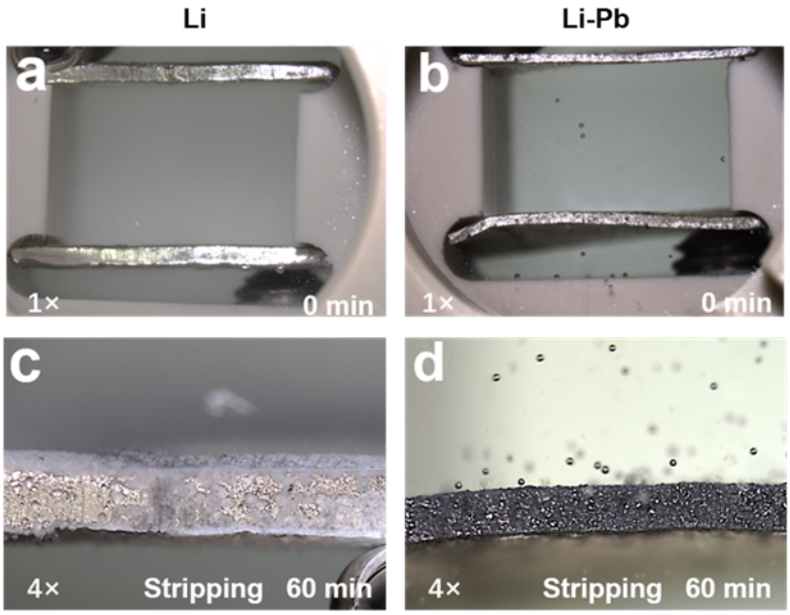

Fig. S 2 Cross-section images of Li and Li-Pb alloys standing (a and b) and stripping at 10 mA cm^{-2} for 10 mAh cm^{-2} (c and d) in in-situ cells.

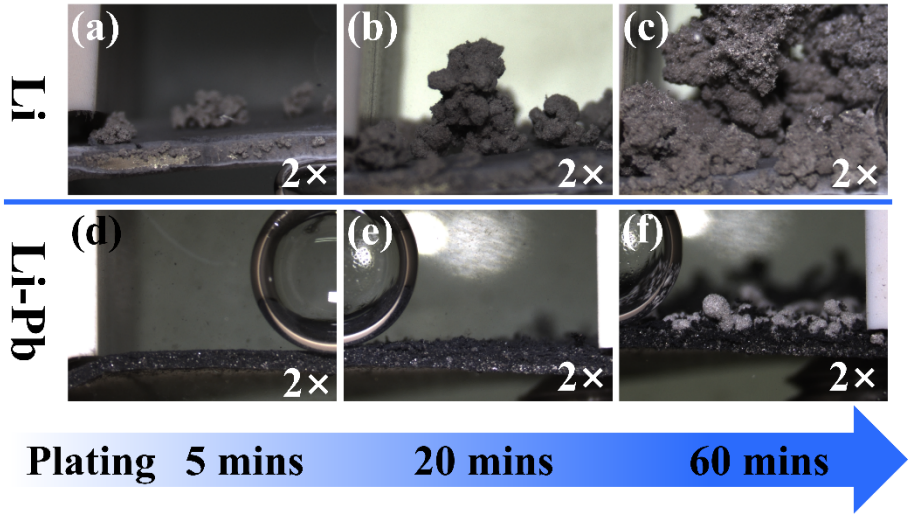

Fig. S 3 Cross-section images of Li (a, b, c) and Li-Pb (d, e, f) alloys after Li stripping for 10 mA h cm^{-2} and plating for 5 mins, 20 mins, and 60 mins at the current density of 10 mA cm^{-2} in in-situ cells.

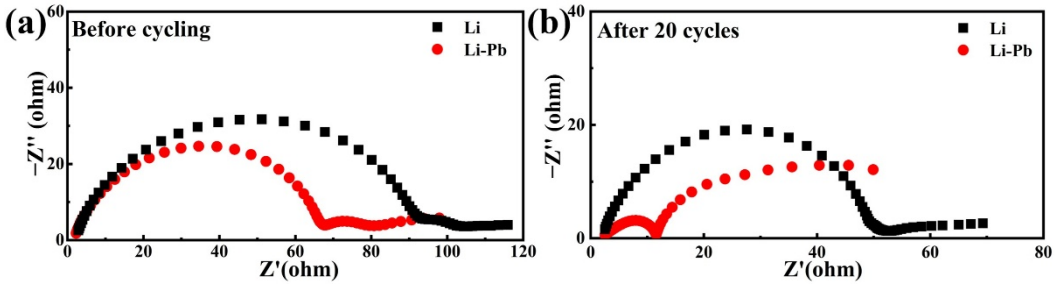

Fig. S 4 Electrochemical impedance spectra of symmetrical cells with different electrodes (a) before cycling and (b) after 20 cycles.

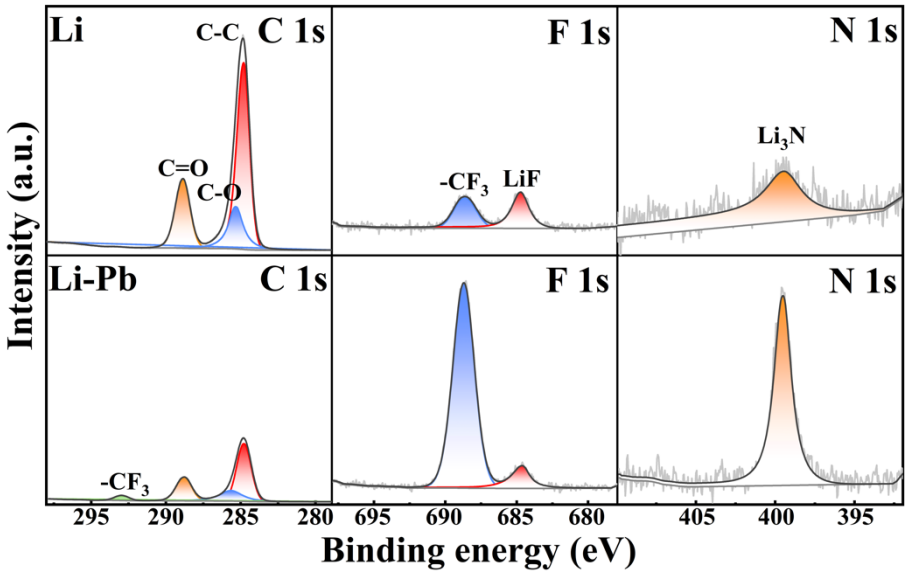

Fig. S 5 C 1s, F 1s and N 1s characteristic peaks of XPS spectra for different electrodes after 20 cycles in symmetrical cells at 0.5 mA cm^{-2} for 0.5 mAh cm^{-2}.

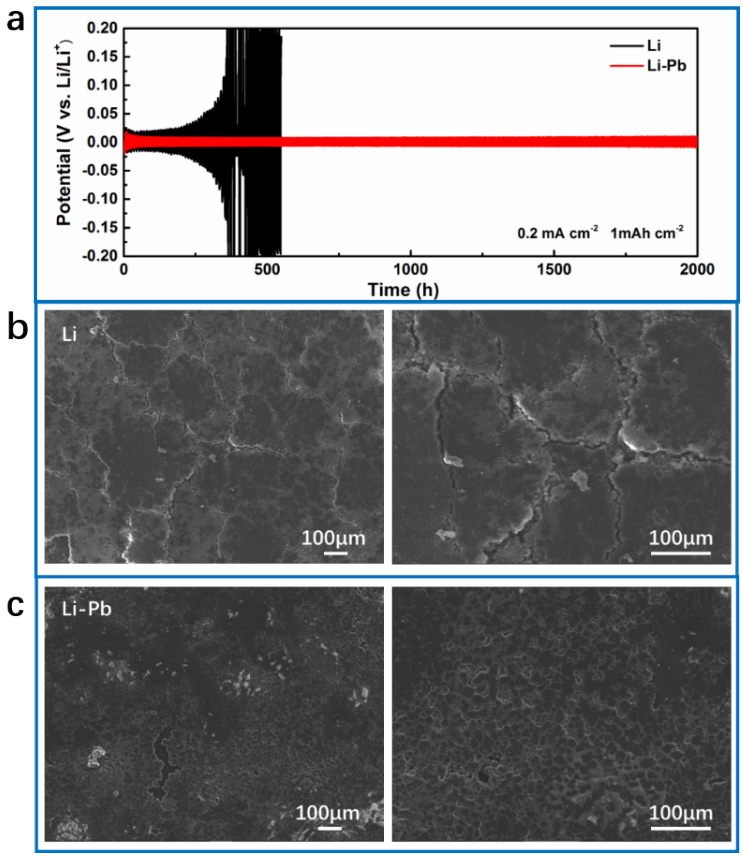

Fig. S 6 (a) Voltage profiles of the Li-Pb and Li-Li symmetric cells at 0.2 mA cm^{-2} for 1 mAh cm^{-2}; SEM images of the (b) Li and (c) Li-Pb alloy anode after cycling for 500 h.

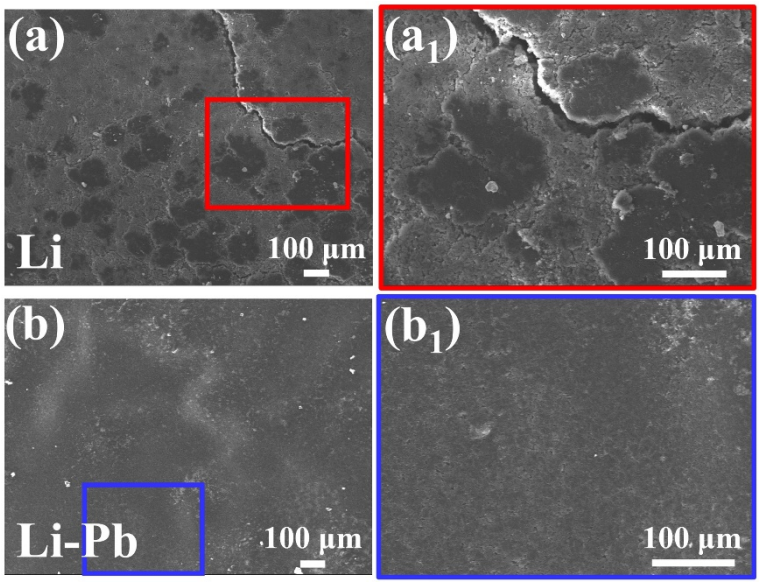

Fig. S 7 The SEM images of the (a and a_1) Li and (b and b_1) Li-Pb alloy electrodes after cycling for 500 h.

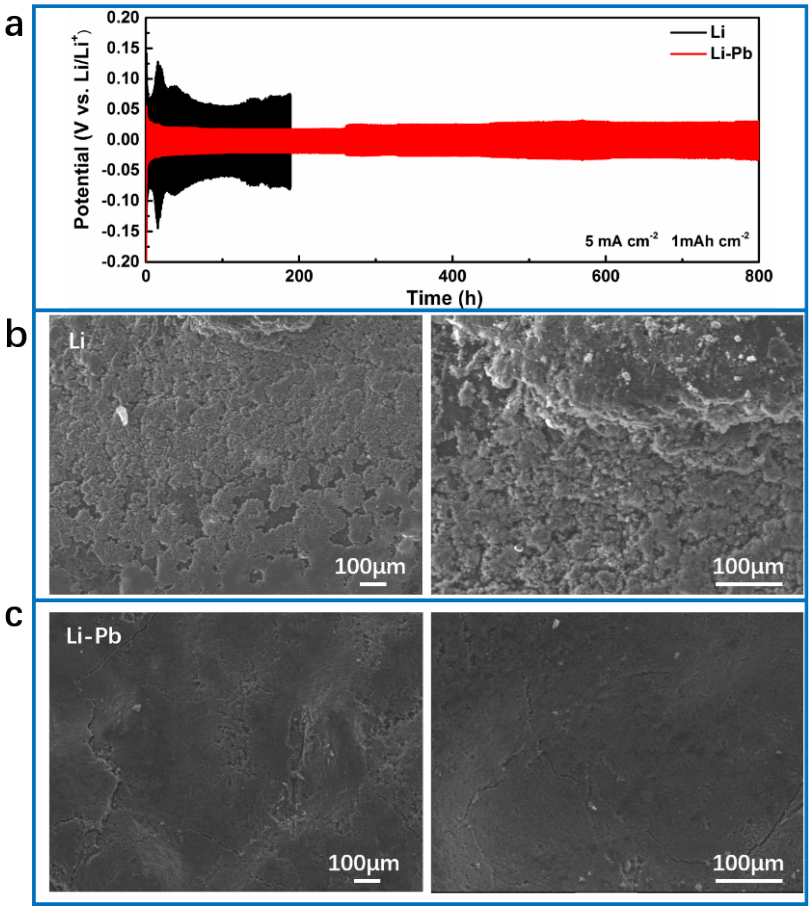

Fig. S 8 (a) Voltage profiles of the Li-Pb and Li-Li symmetric cells at 5 mA cm^{-2} for 1 mAh cm^{-2}; SEM images of the (b) Li and (c) Li-Pb alloy anode after cycling for 500 h.

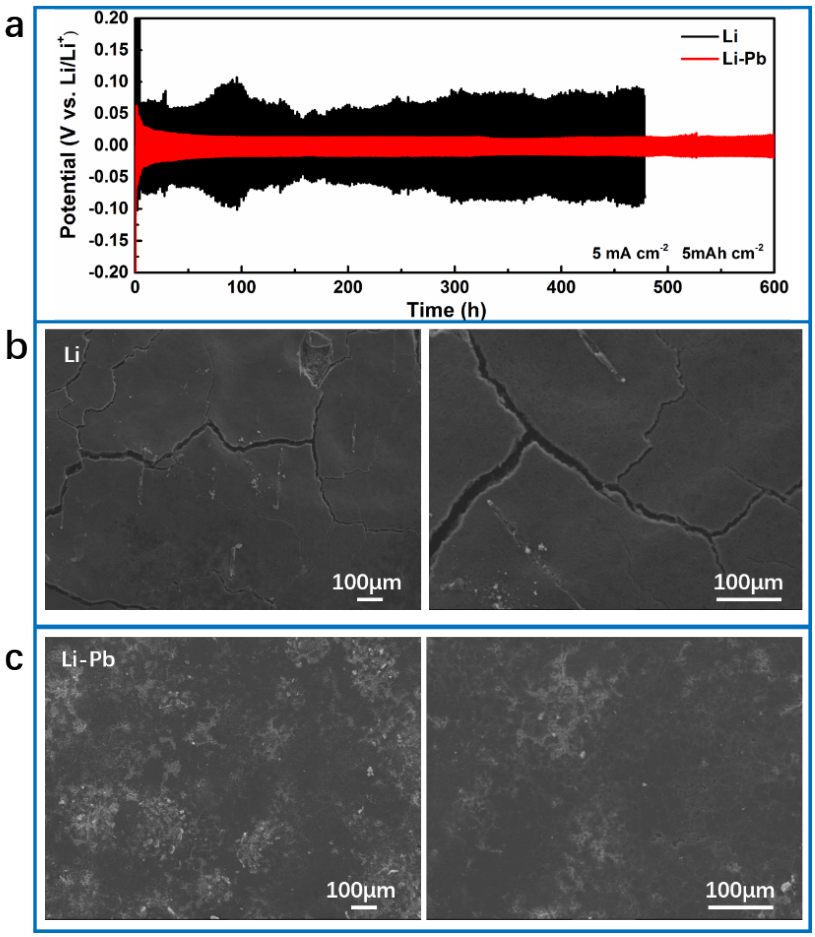

Fig. S 9 (a) Voltage profiles of the Li-Pb and Li-Li symmetric cells at 5mA cm^{-2} for 5 mAh cm^{-2}; SEM images of the (b) Li and (c) Li-Pb alloy anode after cycling for 500 h.

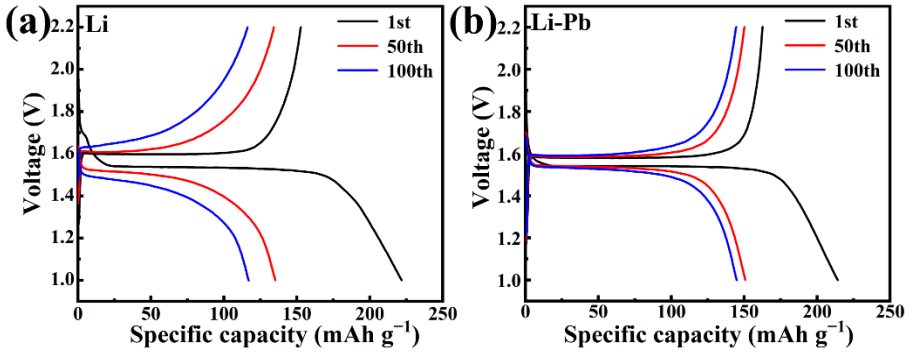

Fig. S 10 The charge-discharge curves (a and b) of the full cells with $Li_4Ti_5O_{12}$ cathodes.